NONLINEAR LOCAL BENDING OF FGM SANDWICH PLATES

Jie Yang, Sritawat Kitipornchai and Kim Meow Liew

NONLINEAR LOCAL BENDING OF FGM SANDWICH PLATES

JIE YANG, SRITAWAT KITIPORNCHAI AND KIM MEOW LIEW

This paper investigates the nonlinear local bending of a sandwich plate consisting of two composite laminated face sheets and a graded core subjected to a lateral patch load. It is assumed that the material composition of the graded layer varies symmetrically along the thickness direction according to a power law distribution. The present analysis is based on the first order shear deformation plate theory and von Karman nonlinear kinematics, with the interaction between the loaded face sheet and the graded core being modeled as an elastic plate resting on a Vlasov-type elastic foundation. A perturbation technique and Galerkin method are used to determine the nonlinear local bending response. Numerical results show that compared with conventional sandwich plates with a homogeneous soft core, the use of a functionally graded core can effectively reduce both the local deformation and interfacial shear stresses. A parametric study is performed to show the influences of the volume fraction index, Young's modulus ratio, thickness of the graded core, boundary condition, and load position.

1. Introduction

Due to their high specific stiffness, light weight, exceptional impact energy absorption, and excellent thermal and acoustical insulation characteristics, sandwich structures are widely used in many engineering applications such as infrastructures, marine constructions, automobiles, and the aerospace industry. A typical sandwich structure consists of two stiff face sheets and a thick intermediate core of low-density and low-modulus material sandwiched in between. One of the major concerns in using such a structure is the so-called "interface problem" (possible crack and delamination at the face sheet/core interfaces caused by the transverse shear stress concentration) that arises from large stiffness differences between the face sheets and the core which may result in a significant deterioration in structure reliability.

Functionally graded materials (FGMs) constitute a new class of inhomogeneous composites whose material composition and physical properties change continuously and smoothly in one or more spatial coordinates so that the interface problem can be effectively mitigated or eliminated. Rapid advances in manufacturing techniques have enabled the fabrication of bulk FGMs that can be used in large-scale structural systems [Ichikawa 2001]. This provides an advantageous degree of freedom in incorporating FGMs into a sandwich structure to achieve a smooth variation in the material property profile. Recent theoretical and experimental investigations [Apetre et al. 2002; Anderson 2003; Venkataraman and Sankar 2003; Venkataraman et al. 2004; Kirugulige et al. 2005; Pollien et al. 2005; Das et al. 2006; Apetre et al. 2006; Zhu and Sankar 2007] have shown that the use of an FGM core can significantly reduce the interfacial shear stresses.

It is known that under a highly localized lateral load such as a point or a patch load, a sandwich structure tends to fail not by overall bending but more often by excessive bending deformation or indentation into the soft core layer around the loaded area. In such a case, the local deformation can be regarded as the relative deflection of the loaded face sheet against the unloaded face sheet. Quite a few theoretical and experimental studies have been conducted to address this issue [Corbett and Reid 1993; Thomsen 1993; Thomsen 1995; Frostig and Baruch 1996; Abrate 1997; da Silva and Santos 1998; Polyakov 2001; Koissin et al. 2004; Hohe and Librescu 2004; Carrera and Ciuffreda 2005], among many others. For sandwich plate structures with a continuous core layer, the relative deflection can be determined by using an approximate approach in which the core layer is modeled as an elastic foundation. Weissman-Berman et al. [1996] treated the loaded face sheet as a Kirchhoff plate resting on a Winkler-type elastic foundation whose equivalent foundation stiffness was dependent on the material properties of the core. For a thick core whose shearing effect is important, Thomsen [1993; 1995] suggested a modified Vlasov-type elastic foundation model and studied the local bending behavior of simply supported rectangular sandwich panels with thin orthotropic face layers. By modeling the sandwich panel as an infinite orthotropic elastic plate resting on a rigid-plastic foundation, Türk and Fatt [1999] investigated the local damage response of a composite sandwich panel induced by static indentation of a hemispherical-nose indenter. It is noted that all of the aforementioned studies were based on the linear displacement-strain relationship only and did not take into account the geometric nonlinearity which is inevitable when a sandwich structure is subjected to a localized load of high density. The only work including this effect was reported by Yang et al. [2001] who presented a nonlinear local bending analysis of composite laminated sandwich plates with a flexible core under a combination of lateral strip load and uniform edge forces by using the classical plate theory and a differential quadrature based semi analytical method. Their results showed that the nonlinear local bending response is considerably different from linear predictions.

This paper investigates the geometrically nonlinear bending response of a rectangular FGM sandwich plate subjected to a lateral patch load within the framework of von Karman-type geometric nonlinearity and the first order shear deformation plate theory. The sandwich plate consists of a thick symmetrically graded core layer bonded by two composite face sheets. The Vlasov-type elastic foundation model is used to describe the supporting action of the graded core to the loaded face sheet. The nonlinear governing partial differential equations are first transformed into a group of linear equations through the use of a perturbation technique and then solved by the Galerkin procedure. Illustrative examples are analyzed to gain an insight into the effects of the Young's modulus ratio, the thickness ratio, the boundary condition as well as the load position on the nonlinear local bending response.

2. Analytical formulations

2.1. *Vlasov-type elastic foundation model.* Figure 1 shows a rectangular sandwich plate of length a and width b consisting of an isotropic inhomogeneous thick core of thickness H_c and two composite laminated face sheets of equal thickness H_f. Let (x, y, z) be a set of coordinates with the x- and y-axes located in the middle plane of the upper face sheet and the z-axis pointing upwards. The material profile of the core changes continuously along the thickness direction according to a power law distribution and is compositionally symmetric about its midplane. The effective Young's modulus at an arbitrary point
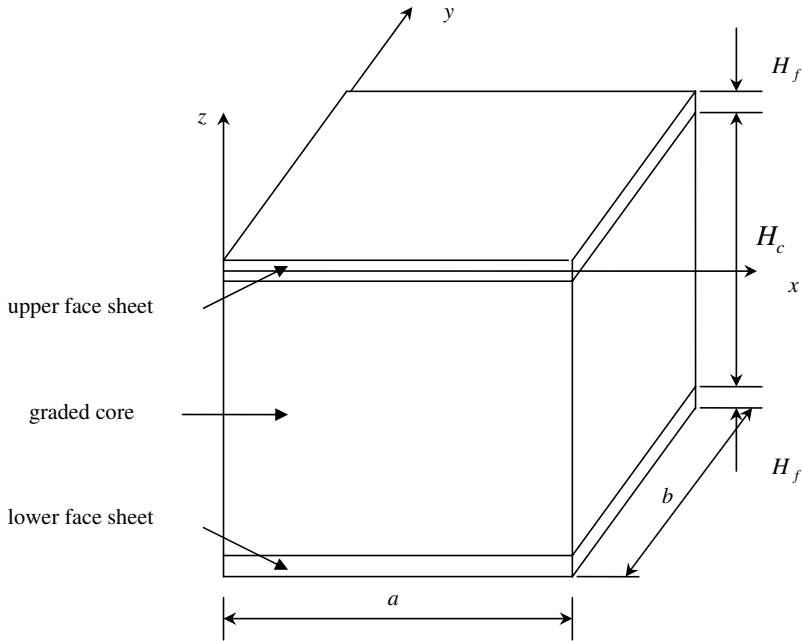
Figure 1. Schematic configuration of an FGM sandwich plate.

within the core layer can be determined by

$$
E_{\text{core}} = \begin{cases} (E_1 - E_0)\left(2\dfrac{z+h}{H_c}\right)^n + E_0 & -h \le z \le -0.5H_f, \\[2mm] (E_1 - E_0)\left(-2\dfrac{z+h}{H_c}\right)^n + E_0 & -h - 0.5H_c \le z \le -h, \end{cases}
\tag{1}
$$

where $h = (H_c + H_f)/2$, n is the non-negative volume fraction index, E_0 denotes the Young's modulus in the mid-plane of the core and is much smaller than the Young's modulus E_1 at the face sheet/core interface. Poisson's ratio is taken to be constant throughout the core ($\nu_{\text{core}} = \nu_0 = \nu_1$).

It is assumed in this study that

(1) the face sheets and the graded core are perfectly bonded so that no separation takes place,

(2) the graded core and the face sheet have the same Young's modulus, that is, $E_1 = E_f$ at the face sheet/core interfaces to achieve a smooth variation in material properties, and

(3) a large value of n is used to obtain a graded soft core whose E_{core} in the majority of the cross section is much smaller than E_f.

Suppose that the upper face sheet is subjected to a lateral patch load $q(x, y) = q_0\varphi(x, y)$ distributed over a small area $2a_q \times 2b_q$ with its center located at (x_q, y_q). q_0 and $\varphi(x, y)$ denote the magnitude and the distribution function of the load. To take into account the shearing effect in the graded core, the interaction between the loaded face sheet and the core layer is modeled by a Vlasov-type two-parameter

foundation as

$$p = K_1 w(x, y) - K_2 \nabla^2 w(x, y), \tag{2}$$

where $w(x, y)$ is the relative deflection of the upper face sheet against the lower face sheet, p is the foundation reaction per unit area provided by the graded core, $\nabla^2 = \partial^2/\partial x^2 + \partial^2/\partial y^2$ is the Laplace operator, K_1 and K_2 are the equivalent spring stiffness and shear stiffness of the foundation which can be derived using Lagrange's principle of virtual work [Selvadurai 1979] as

$$K_1 = \int_{-(h_f/2+H_c)}^{-h_f/2} \frac{\tilde{E}(z)}{[1-\tilde{v}^2]} \left(\frac{d\phi(z)}{dz}\right)^2 dz, \qquad K_2 = \int_{-(h_f/2+H_c)}^{-h_f/2} \frac{\tilde{E}(z)}{4[1+\tilde{v}]} \phi(z)^2 dz, \tag{3}$$

in which $\tilde{E} = E_{core}/(1 - v_{core}^2)$, $\tilde{v} = v_{core}/(1 - v_{core})$, and $\phi(z)$ is the deformation distribution of the core layer that is considered to be in the plane strain state and takes the exponential form

$$\phi(z) = \frac{\sinh[1.5(H_c - z - h)/b]}{\sinh(1.5\,H_c/b)}. \tag{4}$$

It can be seen from the calculations based on Equations (3) and (4) that both K_1 and K_2 fall sharply and then remain almost constant as the volume fraction index n and the modulus ratio E_1/E_0 increase. The variation of K_1 with the core thickness H_c follows almost the same pattern. The value of K_2, however, increases steadily as H_c increases, implying that the shearing effect of the core material tends to be more important for sandwich plates with a thick core.

At the interface between the loaded upper face sheet and the graded core ($z = -0.5H_f$), the stress components σ_z, τ_{zx}, and τ_{zy} can be calculated by

$$\sigma_z|_{z=-0.5H_f} = K_1 w(x, y) - K_2 \nabla^2 w(x, y), \tag{5a}$$

$$\tau_{zx}|_{z=-0.5H_f} = K_2 u(x, y, -0.5H_f), \tag{5b}$$

$$\tau_{zy}|_{z=-0.5H_f} = K_2 v(x, y, -0.5H_f), \tag{5c}$$

where u and v are in-plane displacement components of the loaded face sheet at the interface.

2.2. *Governing equations.* The face sheet considered in this study may be one of the following: (1) an antisymmetrically angle-ply laminated plate; (2) a symmetrically cross-ply laminated plate; or (3) a symmetric angle-ply laminated plate with more than 15 plies. In these cases, the plate stiffness elements $A_{16} = A_{26} = D_{16} = D_{26} = 0$. Both isotropic and orthotropic plates can be treated as special cases.

The first order shear deformation theory is used to account for the transverse shear deformation of the face sheet. Hence, the displacement field (u, v, w) of the loaded face sheet takes the form

$$\begin{Bmatrix} u(x, y, z) \\ v(x, y, z) \\ w(x, y, z) \end{Bmatrix} = \begin{Bmatrix} \bar{u}(x, y) \\ \bar{v}(x, y) \\ \bar{w}(x, y) \end{Bmatrix} + z \begin{Bmatrix} \psi_x(x, y) \\ \psi_y(x, y) \\ 0 \end{Bmatrix}, \tag{6}$$

where $(\bar{u}, \bar{v}, \bar{w})$ are the displacements of a point on the midplane of the face sheet ($z = 0$) and (ψ_x, ψ_y) are cross sectional rotations about the y- and x-axes, respectively.

The partial differential equations governing the nonlinear flexural response of the loaded face sheet in the sense of von Karman-type nonlinear kinematics [Liew et al. 2004] can be written in dimensionless form as

$$L_{11}(U) + L_{12}(V) + L_{14}(\psi_x) + L_{15}(\psi_y) + \mu L_{16}(W, W) = 0, \tag{7}$$

$$L_{21}(U) + L_{22}(V) + L_{24}(\psi_x) + L_{25}(\psi_y) + \mu\beta L_{26}(W, W) = 0, \tag{8}$$

$$L_{33}(W) + L_{34}(\psi_x) + L_{35}(\psi_y) + \mu^2 L_{36}(W, W) + \mu L_{37}[(U, V, \psi_x, \psi_y), W] = \lambda_q \varphi(x, y)/\mu, \tag{9}$$

$$L_{41}(U) + L_{42}(V) - L_{43}(W) + L_{44}(\psi_x) + L_{45}(\psi_y) + \mu L_{46}(W, W) = 0, \tag{10}$$

$$L_{51}(U) + L_{52}(V) - L_{53}(W) + L_{54}(\psi_x) + L_{55}(\psi_y) + \mu L_{56}(W, W) = 0, \tag{11}$$

where the linear partial differential operators L_{ij} $(i, j \leq 5)$, the nonlinear partial differential operators L_{i6} $(i = 1, \ldots, 5)$, and L_{37} are given in the Appendix. The dimensionless quantities in (7)–(11) are

$$\xi = x/a,$$
$$\eta = y/b,$$
$$\beta = a/b,$$
$$\mu = H_f/a,$$
$$(U, V, W) = (\bar{u}, \bar{v}, \bar{w})/H_f,$$
$$(k_1, k_2) = (K_1 a^2, K_2)/A_{11},$$
$$\lambda_q = q_0 a/A_{11},$$
$$(\gamma_1, \gamma_2, \gamma_3) = [A_{44}, A_{45}, A_{55}]H_f^2/D_{11},$$
$$(\gamma_{11}, \gamma_{12}, \gamma_{13}, \gamma_{14}) = [A_{66}, A_{12} + A_{66}, A_{12}, A_{22}]/A_{11},$$
$$(\gamma_{15}, \gamma_{16}, \gamma_{17}, \gamma_{18}, \gamma_{19}, \gamma_{110}, \gamma_{111}) = [B_{11}, B_{16}, B_{66}, B_{12} + B_{66}, B_{26}, B_{22}, B_{12}]/(A_{11}H_f),$$
$$(\gamma_{41}, \gamma_{42}) = [D_{66}, D_{12} + D_{66}]/D_{11},$$
$$(\gamma_{43}, \gamma_{44}, \gamma_{45}, \gamma_{46}, \gamma_{47}, \gamma_{48}) = [B_{11}, B_{16}, B_{66}, B_{12} + B_{66}, B_{26}, B_{22}]H_f/D_{11},$$

in which A_{ij}, B_{ij} and D_{ij} are the stiffness elements of the face sheet

$$(A_{ij}, B_{ij}, D_{ij}) = \sum_{k=1}^{N_L} \int_{z_k}^{z_{k+1}} Q_{ij}^{(k)}(1, z, z^2)dz \qquad (i, j = 1, 2, 4, 5, 6), \tag{12}$$

where $Q_{ij}^{(k)}$ are the reduced stiffnesses for the kth layer of the N_L-ply laminated face sheet and are functions of fiber orientation of that layer. Their expressions are available in many references; see, for example, the book by Reddy [1997].

The edges of the loaded face sheet may be either simply supported or clamped with the boundary conditions

$$W = 0, \qquad \psi_s = 0, \qquad M_n = 0, \qquad N_n = 0, \qquad U_s = 0, \tag{13a}$$

for a simply supported edge, and

$$W = 0, \qquad \psi_s = 0, \qquad \psi_n = 0, \qquad U_n = 0, \qquad U_s = 0, \tag{13b}$$

for a clamped edge. The subscripts n and s refer to the normal and tangential directions of the edge, and N_n, N_{ns}, M_n, M_{ns}, Q_n are the in-plane forces, moments, and transverse shear force, respectively.

3. Analytical methodology

3.1. *Perturbation technique.* To determine the local response of the loaded face sheet, a perturbation technique [Yang et al. 2001; Yang and Shen 2003a; Yang and Shen 2003b] is used, and the unknown displacement components $(U, V, W, \psi_x, \psi_y)$ are expanded in an ascending power series up to the Rth order for a small perturbation parameter λ_q as

$$(U, V, W, \psi_x, \psi_y) = \sum_{r}^{R} (\lambda_q)^r (U^{(r)}, V^{(r)}, W^{(r)}, \psi_x^{(r)}, \psi_y^{(r)}). \tag{14}$$

Following a standard perturbation technique, a set of equations can be obtained in terms of $U^{(r)}$, $V^{(r)}$, $W^{(r)}$, $\psi_x^{(r)}$, and $\psi_y^{(r)}$:

$$L_{11}(U^{(r)}) + L_{12}(V^{(r)}) + L_{14}(\psi_x^{(r)}) + L_{15}(\psi_y^{(r)}) = R_1^{(r)}, \tag{15}$$

$$L_{21}(U^{(r)}) + L_{22}(V^{(r)}) + L_{24}(\psi_x^{(r)}) + L_{25}(\psi_y^{(r)}) = R_2^{(r)}, \tag{16}$$

$$L_{33}(W^{(r)}) + L_{34}(\psi_x^{(r)}) + L_{35}(\psi_y^{(r)}) = R_3^{(r)}, \tag{17}$$

$$L_{41}(U^{(r)}) + L_{42}(V^{(r)}) - L_{43}(W^{(r)}) + L_{44}(\psi_x^{(r)}) + L_{45}(\psi_y^{(r)}) = R_4^{(r)}, \tag{18}$$

$$L_{51}(U^{(r)}) + L_{52}(V^{(r)}) - L_{53}(W^{(r)}) + L_{54}(\psi_x^{(r)}) + L_{55}(\psi_y^{(r)}) = R_5^{(r)}, \tag{19}$$

where

$$R_1^{(1)} = R_2^{(1)} = R_4^{(1)} = R_5^{(1)} = 0, \qquad R_3^{(1)} = \varphi(x, y)/\mu, \tag{20}$$

$$R_i^{(r)} = -\mu \sum_{s=1}^{i-1} L_{i6}(W^{(r-s)}, W^{(s)}) \qquad (r = 2, \ i = 1, 2, 4, 5),$$

$$R_3^{(2)} = -\mu^2 \sum_{s=1}^{i-1} L_{37}[(U^{(r-s)}, V^{(r-s)}, \psi_x^{(r-s)}, \psi_y^{(r-s)}), W^{(s)}],$$

$$R_3^{(r)} = -\mu R_{31}^{(r)} - \mu^2 \sum_{s=1}^{i-1} L_{37}[(U^{(r-s)}, V^{(r-s)}, \psi_x^{(r-s)}, \psi_y^{(r-s)}), W^{(s)}] \quad (r \geq 3). \tag{21}$$

Obviously, the right-hand terms $R_i^{(r)}$ ($i = 1, \ldots, 5$) have already been determined in the previous perturbation step and can be treated as "pseudoloads" at the current step. In (21), the terms $R_{31}^{(r)}$ ($r \geq 3$), up to the fifth-order perturbation, are

$$R_{31}^{(3)} = \left(\frac{\partial^2 W^{(1)}}{\partial \xi^2} + \gamma_{13} \beta^2 \frac{\partial^2 W^{(1)}}{\partial \eta^2} \right) \left(\frac{\partial W^{(1)}}{\partial \xi} \right)^2 + 2\gamma_{11} \beta \frac{\partial^2 W^{(1)}}{\partial \xi \partial \eta} \frac{\partial W^{(1)}}{\partial \xi} \frac{\partial W^{(1)}}{\partial \eta}$$

$$+ \beta^2 \left(\gamma_{13} \frac{\partial^2 W^{(1)}}{\partial \xi^2} + \beta^2 \gamma_{14} \frac{\partial^2 W^{(1)}}{\partial \eta^2} \right) \left(\frac{\partial W^{(1)}}{\partial \eta} \right)^2, \quad (22)$$

$$R_{31}^{(4)} = \left(\frac{\partial^2 W^{(2)}}{\partial \xi^2} + \gamma_{13}\beta^2 \frac{\partial^2 W^{(2)}}{\partial \eta^2} \right) \left(\frac{\partial W^{(1)}}{\partial \xi} \right)^2$$

$$+ 2\gamma_{11}\beta \left(\frac{\partial^2 W^{(2)}}{\partial \xi \partial \eta} \frac{\partial W^{(1)}}{\partial \xi} \frac{\partial W^{(1)}}{\partial \eta} + \frac{\partial^2 W^{(1)}}{\partial \xi \partial \eta} \frac{\partial W^{(2)}}{\partial \xi} \frac{\partial W^{(1)}}{\partial \eta} + \frac{\partial^2 W^{(1)}}{\partial \xi \partial \eta} \frac{\partial W^{(1)}}{\partial \xi} \frac{\partial W^{(2)}}{\partial \eta} \right)$$

$$+ \beta^2 \left(\gamma_{13} \frac{\partial^2 W^{(2)}}{\partial \xi^2} + \beta^2 \gamma_{14} \frac{\partial^2 W^{(2)}}{\partial \eta^2} \right) \left(\frac{\partial W^{(1)}}{\partial \eta} \right)^2, \quad (23)$$

$$R_{31}^{(5)} = \left(\frac{\partial^2 W^{(1)}}{\partial \xi^2} + \gamma_{13}\beta^2 \frac{\partial^2 W^{(1)}}{\partial \eta^2} \right) \left(\frac{\partial W^{(2)}}{\partial \xi} \right)^2 + \left(\frac{\partial^2 W^{(3)}}{\partial \xi^2} + \gamma_{13}\beta^2 \frac{\partial^2 W^{(3)}}{\partial \eta^2} \right) \left(\frac{\partial W^{(1)}}{\partial \xi} \right)^2$$

$$+ 2\gamma_{11}\beta \left(\frac{\partial^2 W^{(3)}}{\partial \xi \partial \eta} \frac{\partial W^{(1)}}{\partial \xi} \frac{\partial W^{(1)}}{\partial \eta} + \frac{\partial^2 W^{(1)}}{\partial \xi \partial \eta} \frac{\partial W^{(3)}}{\partial \xi} \frac{\partial W^{(1)}}{\partial \eta} + \frac{\partial^2 W^{(1)}}{\partial \xi \partial \eta} \frac{\partial W^{(1)}}{\partial \xi} \frac{\partial W^{(3)}}{\partial \eta} \right.$$

$$\left. + \frac{\partial^2 W^{(2)}}{\partial \xi \partial \eta} \frac{\partial W^{(2)}}{\partial \xi} \frac{\partial W^{(1)}}{\partial \eta} + \frac{\partial^2 W^{(2)}}{\partial \xi \partial \eta} \frac{\partial W^{(1)}}{\partial \xi} \frac{\partial W^{(2)}}{\partial \eta} + \frac{\partial^2 W^{(1)}}{\partial \xi \partial \eta} \frac{\partial W^{(2)}}{\partial \xi} \frac{\partial W^{(2)}}{\partial \eta} \right)$$

$$+ \beta^2 \left(\gamma_{13} \frac{\partial^2 W^{(1)}}{\partial \xi^2} + \beta^2 \gamma_{14} \frac{\partial^2 W^{(1)}}{\partial \eta^2} \right) \left(\frac{\partial W^{(2)}}{\partial \eta} \right)^2 + \beta^2 \left(\gamma_{13} \frac{\partial^2 W^{(3)}}{\partial \xi^2} + \beta^2 \gamma_{14} \frac{\partial^2 W^{(3)}}{\partial \eta^2} \right) \left(\frac{\partial W^{(1)}}{\partial \eta} \right)^2. \quad (24)$$

3.2. *Solution procedure.* The solutions of the perturbation equations (15)–(19) under the associated boundary conditions in (13) can be expanded in series form:

$$U^{(r)} = \sum_{m=1}^{M} \sum_{n=1}^{N} a_{mn}^{(r)} \bar{U}_m(\xi) \tilde{U}_n(\eta), \qquad V^{(r)} = \sum_{m=1}^{M} \sum_{n=1}^{N} b_{mn}^{(r)} \bar{V}_m(\xi) \tilde{V}_n(\eta), \qquad (25a)$$

$$W^{(r)} = \sum_{m=1}^{M} \sum_{n=1}^{N} c_{mn}^{(r)} \bar{W}_m(\xi) \tilde{W}_n(\eta), \qquad \psi_x^{(r)} = \sum_{m=1}^{M} \sum_{n=1}^{N} d_{mn}^{(r)} \bar{\psi}_{xm}(\xi) \tilde{\psi}_{xn}(\eta), \qquad (25b)$$

$$\psi_y^{(r)} = \sum_{m=1}^{M} \sum_{n=1}^{N} e_{mn}^{(r)} \bar{\psi}_{ym}(\xi) \tilde{\psi}_{yn}(\eta), \qquad (25c)$$

where $(a_{mn}^{(r)}, b_{mn}^{(r)}, c_{mn}^{(r)}, d_{mn}^{(r)}, e_{mn}^{(r)})$ are constants to be determined, $(\bar{U}_m^{(r)}, \bar{V}_m^{(r)}, \bar{W}_m^{(r)}, \bar{\psi}_{xm}^{(r)}, \bar{\psi}_{ym}^{(r)})$ and $(\tilde{U}_n^{(r)}, \tilde{V}_n^{(r)}, \tilde{W}_n^{(r)}, \tilde{\psi}_{xn}^{(r)}, \tilde{\psi}_{yn}^{(r)})$ are the analytical functions that satisfy boundary conditions at edges $\xi = 0, 1$ and $\eta = 0, 1$, respectively. For example, when the face sheet is simply supported at $\xi = 0, 1$,

$$\bar{V}_m^{(r)}(\xi) = \bar{W}_m^{(r)}(\xi) = \bar{\psi}_{ym}^{(r)}(\xi) = \sin(m\pi\xi), \qquad \bar{U}_m^{(r)}(\xi) = \bar{\psi}_{xm}^{(r)}(\xi) = \cos(m\pi\xi), \qquad (26)$$

and when the face sheet is clamped at $\xi = 0, 1$,

$$\bar{U}_m^{(r)}(\xi) = \bar{W}_m^{(r)}(\xi) = \bar{\psi}_{ym}^{(r)}(\xi) = X_m(\xi), \qquad \bar{V}_m^{(r)}(\xi) = \bar{\psi}_{xm}^{(r)}(\xi) = \frac{dX_m(\xi)}{d\xi}, \qquad (27)$$

where

$$X_m(\xi) = \sin \mu_m \xi - \sinh \mu_m \xi - \theta_m (\cos \mu_m \xi - \cosh \mu_m \xi),$$

$$\theta_m = (\sin \mu_m - \sinh \mu_m)/(\cos \mu_m - \cosh \mu_m),$$

$$\mu_m = (2m+1)\pi/2.$$

Substituting (25) into the perturbation equations (15)–(19) and applying the Galerkin approach to minimize the residual within the face sheet domain leads to a system of linear algebraic equations from which the constants $(a_{mn}^{(r)}, b_{mn}^{(r)}, c_{mn}^{(r)}, d_{mn}^{(r)}, e_{mn}^{(r)})$ can be determined step by step. Finally, the nonlinear load-deflection relationship for a given point p can be obtained by using the relationship in (14) as

$$W_p = \lambda_q W_p^{(1)} + \lambda_q^2 W_p^{(2)} + \cdots + \lambda_q^R W_p^{(R)}, \tag{28}$$

where W_p refers to the dimensionless deflection at point p.

4. Numerical results and discussions

In the following computations, we use third order perturbation and the condition that $M = N = 5$ in the solution series in Equation (25). These conditions were chosen based on the convergence study implemented by means of varying the total number of series terms and increasing the perturbation order.

To validate the present analysis, the linear local bending of a clamped sandwich plate with a PVC core and orthotropic face sheets subjected to a point load $P = 1\,\text{kN}$ at the plate center is considered. This example was previously analyzed by Thomsen [1993] based on the classical plate theory as well. The geometry and material properties are $a = b = 500\,\text{mm}$, $H_f = 3\,\text{mm}$, $E_{11}^f = 33.6\,\text{GPa}$, $E_{22}^f = 8.4\,\text{GPa}$, $G_{12}^f = 3.1\,\text{GPa}$, $v_{12}^f = 0.32$ for the orthotropic face sheet and $H_c = 30\,\text{mm}$, $E_c = 0.1\,\text{GPa}$, $v_c = 0.35$ for the PVC core. Figure 2 displays the lateral deflection profile at the midspan ($y = b/2$) of the plate. Severe deformation localization can be observed. The deflection reaches its peak value at the center of the plate, and then decays steeply as the distance from the center increases. Good agreement is achieved between the present solution and the finite element method (FEM) results [Thomsen 1993].

The second comparison example concerns the nonlinear bending of a simply supported functionally graded square plate ($a = b = 200\,\text{mm}$, $h = 10\,\text{mm}$) under a uniform lateral pressure of intensity q. The plate is made of a mixture of aluminum ($E = 70\,\text{GPa}$, $v = 0.3$) and zirconia ($E = 151\,\text{GPa}$, $v = 0.3$). Figure 3 presents the curves of dimensionless central deflection $w_0 = w/h$ versus load parameter $q^* = qa^4/E_m h^4$ for plates with different material compositions where E_m is the Young's modulus of aluminum. The FEM results [Reddy 2000] based on the higher-order shear deformation plate theory are also provided for direct comparison. Again, good agreement is observed. The discrepancy in the above comparisons is due to the different numerical solution methods used in the present analysis and existing studies [Thomsen 1993; Reddy 2000].

Figures 4–9 give the numerical results for square sandwich plates with a symmetrically graded core and 4-layer ($-45°/45°/-45°/45°$) antisymmetric angle-ply Kevlar/epoxy face sheets of equal ply thickness. Unless stated otherwise, the plate is assumed to be simply supported at all sides and subjected to a uniformly distributed patch load over an area $(2a_q, 2b_q) = (2 \times 0.05a, 2 \times 0.05b)$ in the vicinity of the center of the plate $(x_q, y_q) = (0.5a, 0.5b)$. The material properties and geometrical parameters are: $E_{11}^f = 76\,\text{GPa}$, $E_{22}^f = 5.5\,\text{GPa}$, $G_{12}^f = 2.3\,\text{GPa}$, $v_{12}^f = 0.34$, $H_f = 5\,\text{mm}$, $a = b = 500\,\text{mm}$ for the face
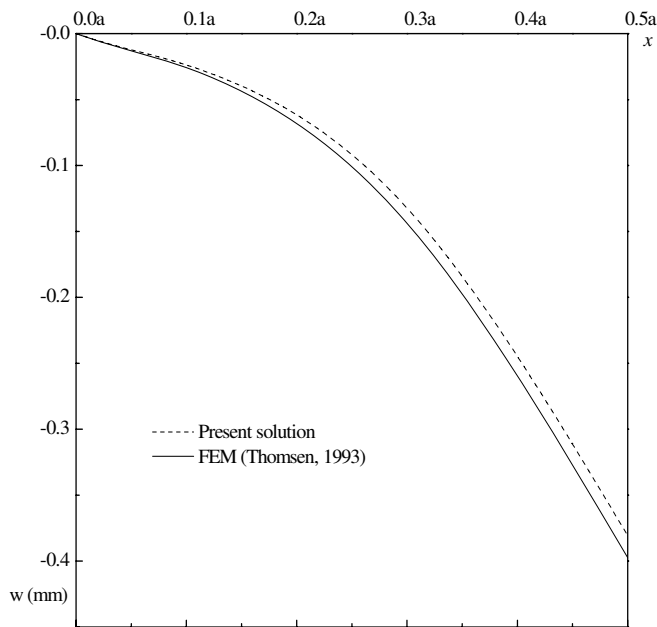
Figure 2. Comparison of the linear deflection profile $w|_{y=0.5b}$ of an orthotropic loaded face sheet under a point load at the plate center.
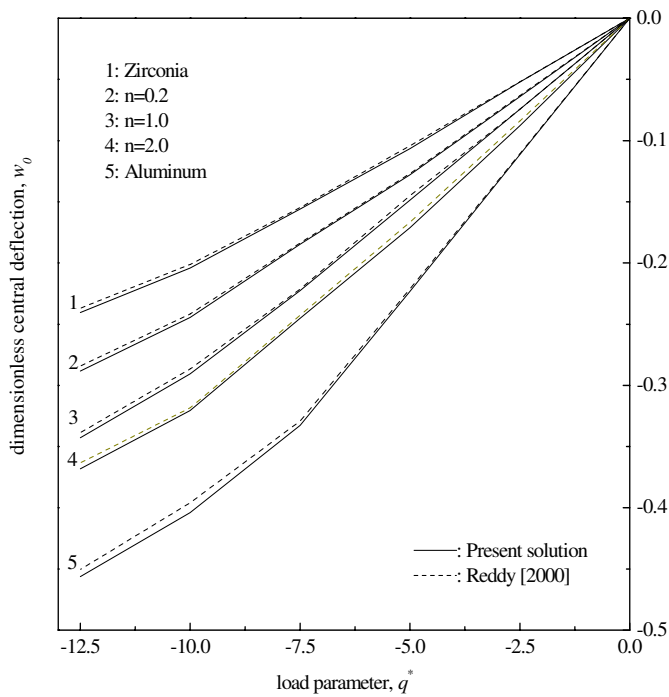
Figure 3. Nonlinear load-deflection curves of simply supported FGM square plates under uniform lateral pressure.
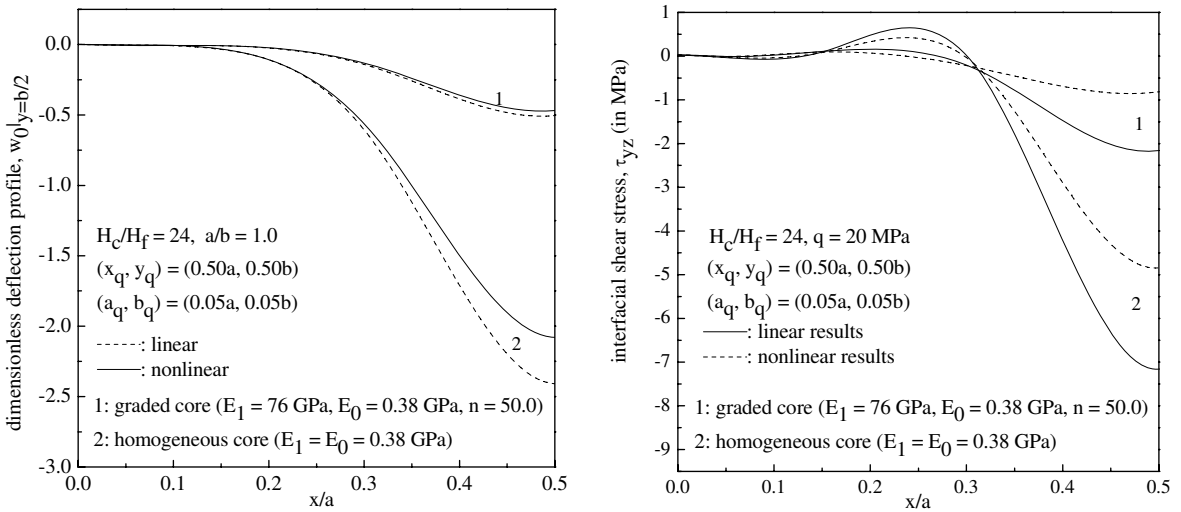
Figure 4. Comparison of the nonlinear local bending response of square sandwich plates with a homogeneous core and a graded core: (left) deflection profile $w_0|_{y=b/2}$; (right) interface shear stress $\tau_{yz}|_{y=b/2}$.

sheet, and $E_1 = 76\,\text{GPa}$, $E_1/E_0 = 200$, $\nu = 0.08$, $H_c/H_f = 24$, $n = 50.0$ for the graded core. The load intensity is $q = 20\,\text{MPa}$ in Figures 4 and 9 and can vary up to $q = 40\,\text{MPa}$ in other examples. Numerical results of normalized deflection $w_0 = w/H_f$ and stresses (in MPa) at the loaded upper face sheet/graded core interface are provided.

We first compare the local deflection profiles and interfacial transverse shear stress distributions of sandwich plates with a graded core ($E_1 = 76\,\text{GPa}$, $E_0 = 0.38\,\text{GPa}$, $n = 50.0$) and with a homogeneous soft core ($E_1 = E_0 = 0.38\,\text{GPa}$) subjected to a patch load $q = 20\,\text{MPa}$. Due to the symmetry in both structural configuration and loading condition, only the deformed shape and shear stress τ_{yz} at the midspan $y = b/2$ on the left half of the plate are displayed in Figure 4 where nonlinear and linear results are represented by solid and dashed curves, respectively. The local deflection and the interfacial shear stress τ_{yz} are maximal at the plate center and decay rapidly towards the plate edge. It is important to note that both deflection and interfacial shear stress τ_{yz} are greatly reduced when a graded core is used. This is because the equivalent supporting stiffnesses K_1 and K_2 of the graded core are significantly higher than those of a homogeneous core. This observation is of particular importance since it indicates that the structural performance of a sandwich plate can be effectively improved through the use of a graded core that is capable of alleviating the local deformation and lowering the interfacial shear stress responsible for debonding failure at the face sheet/core interface.

Figure 5 displays the load-central deflection curves and the load-central interfacial stress curves for sandwich plates with a homogeneous soft core ($E_1 = E_0 = 0.38\,\text{GPa}$) and a graded core with varying volume fraction index ($E_1/E_0 = 200$, $E_1 = 76\,\text{GPa}$, $n = 20, 50$). It should be noted that under the power law defined in Equation (1), the graded core becomes stiffer as the volume fraction index n decreases, while $n = \infty$ corresponds to a core that is roughly homogeneous. Because of this, the sandwich plate with a graded core of $n = 20$ has the lowest central deflection. An increase in n leads to a higher τ_{yz} but
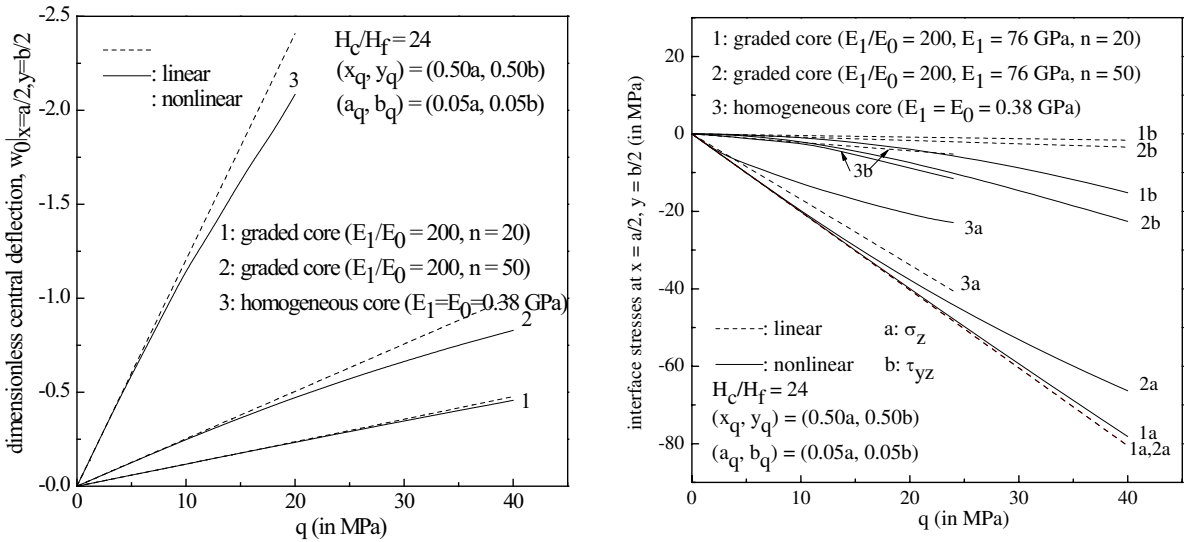
Figure 5. Comparison of the nonlinear local bending response of square sandwich plates with a homogeneous core and a graded core: (left) load-central deflection curves; (right) load-central interface stress curves.

a lower σ_z. As can be observed in Figures 4 and 5, linear solutions greatly overpredict the deflection and interfacial normal stress σ_z but on the other hand, considerably underestimate the interfacial shear stress τ_{yz}. This discrepancy becomes even more significant when a graded core with a larger value of n is used. Note that for the sandwich plate with $n = 20$, the load-central interfacial normal stress σ_z relationship is basically linear. This is due to the fact that its load-central deflection curve is almost linear and the first term in Equation (5a), which has a much higher weighing than the second term, is directly proportional to the deflection.

To investigate the effect of modulus ratio E_1/E_0 of the graded core, the nonlinear load-central deflection and load-central interfacial stress curves for sandwich plates containing a graded core ($n = 50$) with $E_1/E_0 = 100, 500,$ and 1000 are given in Figure 6. The Young's modulus at the face sheet/core interface E_1 is kept constant, while that at the core center E_0 is varied. Therefore, a larger E_1/E_0 ratio in fact indicates a softer graded core with a smaller E_0. The nonlinear deflection and interfacial shear stress τ_{yz} increase, whereas the interfacial normal stress σ_z decreases as the E_1/E_0 ratio is increased. It is worth noting that the results for $E_1/E_0 = 500$ and 1000 are quite close, implying that the nonlinear local response will almost not be affected by the change of E_1/E_0 beyond a certain value, say, $E_1/E_0 \geq 500$ in this example.

Figure 7 examines the influence of the thickness ratio H_c/H_f on the nonlinear local bending behavior of FGM sandwich plates. It is assumed that only the core thickness H_c is changed, while the face sheet thickness remains constant. Both the central deflection and central interfacial stresses follow a nonmonotonic variation with the core thickness. A sandwich plate with $H_c/H_f = 30$ has the greatest
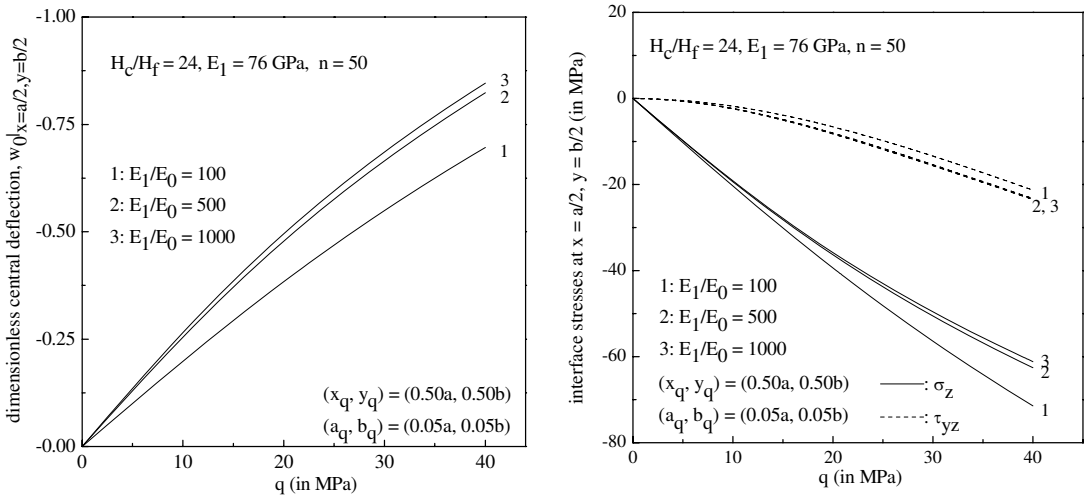
Figure 6. Nonlinear local bending response of square FGM sandwich plates with different E_1/E_0 ratios: (left) load-central deflection curves; (right) load-central interface stress curves.
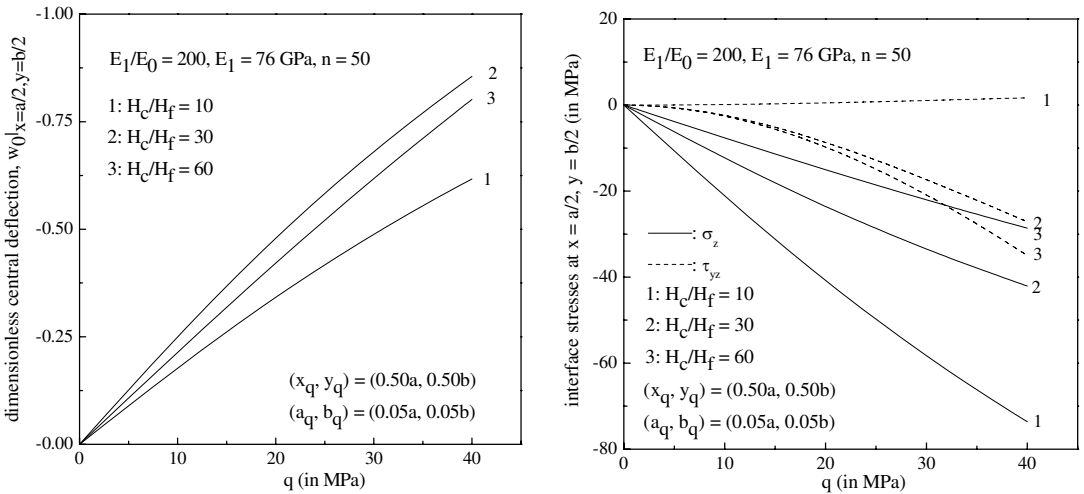
Figure 7. Nonlinear local bending response of square FGM sandwich plates with different H_c/H_f ratios: (left) load-central deflection curves; (right) load-central interface stress curves.

central deflections, but its central interfacial stresses are intermediate to those of the plates with $H_c/H_f = 10$ and $H_c/H_f = 60$. The reason is that as the graded core becomes thicker the spring stiffness K_1 becomes smaller but the shear stiffness K_2 becomes larger, and the local bending behavior of the plate depends largely on the combined effects of foundation stiffnesses K_1 and K_2.

The nonlinear local bending responses of FGM sandwich plates under different boundary conditions are depicted in Figure 8 in which notations "SSSS", "CCCC" and "SCSC" stand for, respectively, a simply
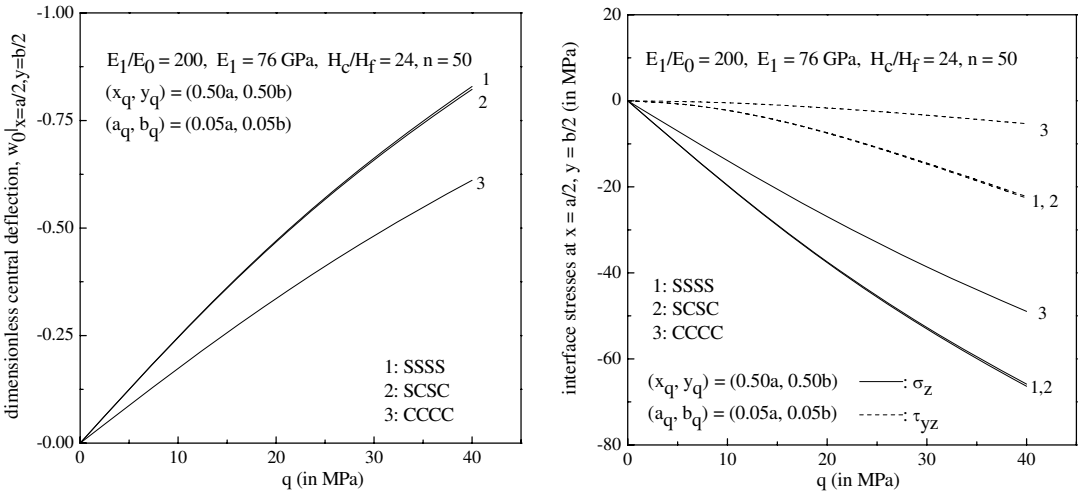
Figure 8. Nonlinear local bending response of square FGM sandwich plates with different boundary conditions: (left) load-central deflection curves; (right) load-central interface stress curves.
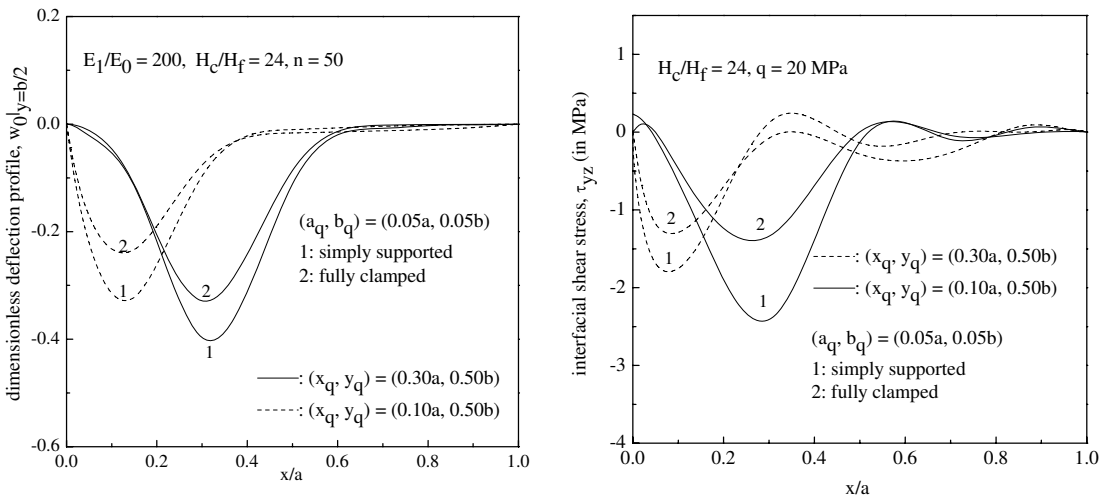
Figure 9. Effect of load position on: (left) the dimensionless central deflection profile $w_0|_{y=b/2}$; and (b) the interface shear stress $\tau_{yz}|_{y=b/2}$ of a square FGM sandwich plate.

supported sandwich plate, a clamped sandwich plate, and a sandwich plate clamped at edges $x = 0$, a and simply supported at edges $y = 0$, b. The results show that the boundary constraints have a significant effect on the nonlinear local bending response. The fully clamped plate undergoes the lowest nonlinear deflection and interfacial stresses. The nonlinear local responses of the SSSS and SCSC sandwich plates are almost identical.

Figure 9 gives the deflection profiles and interfacial shear stress distributions for simply supported and clamped FGM sandwich plates under a patch load $q = 20$ MPa centered some distance away from the

plate center ($x_q = 0.1a$, $0.3a$, $y_q = 0.50b$). As can be observed, both the deflection and interface shear stress are affected by the load location. In particular, their peak values, which are of the greatest interest in engineering design, are sensitive to both load location and the boundary conditions. As the load center moves towards the support, both the deformed zone and the peak of interfacial stress distributions shift towards the support accordingly.

5. Concluding remarks

The nonlinear local bending response of a composite sandwich plate containing a functionally graded core under a lateral patch load is investigated based on the first order shear deformation plate theory and von Karman type geometric nonlinearity. The analysis employs a Vlasov-type elastic foundation model including the shear effect in the flexible core to model the interaction between the loaded face sheet and the supporting core, and makes use of a perturbation technique and Galerkin approach to obtain the numerical solutions. It is found that the deformation localization and interfacial transverse shear stress concentration can be effectively reduced by using a core with smooth gradient in material properties. The geometrical nonlinear effect is pronounced at high load levels and must be taken into consideration for a reliable analysis. The use of a graded core with a smaller volume fraction index and a lower modulus ratio E_1/E_0 helps suppress both the nonlinear local deflection and interfacial transverse shear stress but leads to a higher interfacial normal stress. The nonlinear response is significantly influenced by the thickness ratio in a nonmonotonic way and is sensitive to boundary conditions as well.

Appendix

Let $\kappa = \frac{5}{6}$ be the shear correction factor. The linear and nonlinear partial differential operators in Equations (7)–(11) are

$$L_{11} = \frac{\partial^2}{\partial \xi^2} + \beta^2 \gamma_{11} \frac{\partial^2}{\partial \eta^2}, \qquad\qquad L_{12} = L_{21} = \gamma_{12} \beta \frac{\partial^2}{\partial \xi \partial \eta},$$

$$L_{14} = \gamma_{15} \frac{\partial^2}{\partial \xi^2} + 2\gamma_{16} \beta \frac{\partial^2}{\partial \xi \partial \eta} + \gamma_{17} \beta^2 \frac{\partial^2}{\partial \eta^2}, \qquad L_{15} = L_{24} = \gamma_{16} \frac{\partial^2}{\partial \xi^2} + \gamma_{18} \beta \frac{\partial^2}{\partial \xi \partial \eta} + \gamma_{19} \beta^2 \frac{\partial^2}{\partial \eta^2},$$

$$L_{16}(W, W) = \left(\frac{\partial^2 W}{\partial \xi^2} + \gamma_{11} \beta^2 \frac{\partial^2 W}{\partial \eta^2} \right) \frac{\partial W}{\partial \xi} + \gamma_{12} \beta^2 \frac{\partial W}{\partial \xi \partial \eta} \frac{\partial W}{\partial \eta}, \qquad L_{22} = \gamma_{11} \frac{\partial^2}{\partial \xi^2} + \beta^2 \gamma_{14} \frac{\partial^2}{\partial \eta^2},$$

$$L_{25} = \gamma_{17} \frac{\partial^2}{\partial \xi^2} + 2\gamma_{19} \beta \frac{\partial^2}{\partial \xi \partial \eta} + \gamma_{110} \beta^2 \frac{\partial^2}{\partial \eta^2}, \quad L_{26}(W, W) = \left(\gamma_{11} \frac{\partial^2 W}{\partial \xi^2} + \beta^2 \frac{\partial^2 W}{\partial \eta^2} \right) \frac{\partial W}{\partial \eta} + \gamma_{12} \frac{\partial W}{\partial \xi \partial \eta} \frac{\partial W}{\partial \xi},$$

$$L_{33} = \kappa^2 \left(\gamma_3 \frac{\partial^2}{\partial \xi^2} + 2\gamma_2 \beta \frac{\partial^2}{\partial \xi \partial \eta} + \gamma_1 \beta^2 \frac{\partial^2}{\partial \eta^2} \right) + k_1 - k_2 \left(\frac{\partial^2}{\partial \xi^2} + \beta^2 \frac{\partial^2}{\partial \eta^2} \right),$$

$$L_{34} = L_{43} = \frac{\kappa^2}{\mu} \left(\gamma_3 \frac{\partial}{\partial \xi} + \gamma_2 \beta \frac{\partial}{\partial \eta} \right), \qquad\qquad L_{35} = L_{53} = \frac{\kappa^2}{\mu} \left(\gamma_2 \frac{\partial}{\partial \xi} + \gamma_1 \beta \frac{\partial}{\partial \eta} \right),$$

$$L_{36}(W, W)$$
$$= \left(\frac{\partial^2 W}{\partial \xi^2} + \gamma_{13} \beta^2 \frac{\partial^2 W}{\partial \eta^2} \right) \left(\frac{\partial W}{\partial \xi} \right)^2 + 2\gamma_{11} \beta \frac{\partial^2 W}{\partial \xi \partial \eta} \frac{\partial W}{\partial \xi} \frac{\partial W}{\partial \eta} + \beta^2 \left(\gamma_{13} \frac{\partial^2 W}{\partial \xi^2} + \beta^2 \gamma_{14} \frac{\partial^2 W}{\partial \eta^2} \right) \left(\frac{\partial W}{\partial \eta} \right)^2,$$

$$L_{37}[(U, V, \psi_x, \psi_y), W] = \left(\frac{\partial U}{\partial \xi} + \gamma_{13}\beta \frac{\partial V}{\partial \eta} + \gamma_{15} \frac{\partial \psi_x}{\partial \xi} + \gamma_{16}\beta \frac{\partial \psi_x}{\partial \eta} + \gamma_{16} \frac{\partial \psi_y}{\partial \xi} + \gamma_{111}\beta \frac{\partial \psi_y}{\partial \eta} \right) \frac{\partial^2 W}{\partial \xi^2}$$

$$+ 2\beta \left(\gamma_{11}\beta \frac{\partial U}{\partial \eta} + \gamma_{11} \frac{\partial V}{\partial \xi} + \gamma_{16} \frac{\partial \psi_x}{\partial \xi} + \gamma_{17}\beta \frac{\partial \psi_x}{\partial \eta} + \gamma_{17} \frac{\partial \psi_y}{\partial \xi} + \gamma_{19}\beta \frac{\partial \psi_y}{\partial \eta} \right) \frac{\partial^2 W}{\partial \xi \partial \eta}$$

$$+ \beta^2 \left(\gamma_{13} \frac{\partial U}{\partial \xi} + \gamma_{14}\beta \frac{\partial V}{\partial \eta} + \gamma_{111} \frac{\partial \psi_x}{\partial \xi} + \gamma_{19}\beta \frac{\partial \psi_x}{\partial \eta} + \gamma_{19} \frac{\partial \psi_y}{\partial \xi} + \gamma_{110}\beta \frac{\partial \psi_y}{\partial \eta} \right) \frac{\partial^2 W}{\partial \eta^2},$$

$$L_{41} = \gamma_{44} \frac{\partial^2}{\partial \xi^2} + 2\gamma_{45}\beta \frac{\partial^2}{\partial \xi \partial \eta} + \gamma_{46}\beta^2 \frac{\partial^2}{\partial \eta^2}, \qquad L_{42} = L_{51} = \gamma_{45} \frac{\partial^2}{\partial \xi^2} + \gamma_{47}\beta \frac{\partial^2}{\partial \xi \partial \eta} + \gamma_{48}\beta^2 \frac{\partial^2}{\partial \eta^2},$$

$$L_{44} = \frac{\partial^2}{\partial \xi^2} + \beta^2 \gamma_{41} \frac{\partial^2}{\partial \eta^2} - \left(\frac{\kappa}{\mu} \right)^2 \gamma_3, \qquad L_{45} = L_{54} = \gamma_{42}\beta \frac{\partial^2}{\partial \xi \partial \eta} - \left(\frac{\kappa}{\mu} \right)^2 \gamma_2,$$

$$L_{46}(W, W) = \left(\gamma_{44} \frac{\partial^2 W}{\partial \xi^2} + 2\gamma_{45}\beta \frac{\partial^2 W}{\partial \xi \partial \eta} + \gamma_{46}\beta^2 \frac{\partial^2 W}{\partial \eta^2} \right) \frac{\partial W}{\partial \xi} + \beta \left(\gamma_{45} \frac{\partial^2 W}{\partial \xi \partial \eta} + \gamma_{47}\beta \frac{\partial^2 W}{\partial \xi \partial \eta} + \gamma_{48}\beta^2 \frac{\partial^2 W}{\partial \eta^2} \right) \frac{\partial W}{\partial \eta},$$

$$L_{52} = \gamma_{46} \frac{\partial^2}{\partial \xi^2} + 2\gamma_{48}\beta \frac{\partial^2}{\partial \xi \partial \eta} + \gamma_{49}\beta^2 \frac{\partial^2}{\partial \eta^2}, \qquad L_{55} = \gamma_{41} \frac{\partial^2}{\partial \xi^2} + \beta^2 \gamma_{43} \frac{\partial^2}{\partial \eta^2} - \left(\frac{\kappa}{\mu} \right)^2 \gamma_1,$$

$$L_{56}(W, W) = \left(\gamma_{45} \frac{\partial^2 W}{\partial \xi^2} + \gamma_{47}\beta \frac{\partial^2 W}{\partial \xi \partial \eta} + \gamma_{48}\beta^2 \frac{\partial^2 W}{\partial \eta^2} \right) \frac{\partial W}{\partial \xi} + \beta \left(\gamma_{46} \frac{\partial^2 W}{\partial \xi \partial \eta} + 2\gamma_{48}\beta \frac{\partial^2 W}{\partial \xi \partial \eta} + \gamma_{49}\beta^2 \frac{\partial^2 W}{\partial \eta^2} \right) \frac{\partial W}{\partial \eta}.$$

References

[Abrate 1997] S. Abrate, "Localized impact on sandwich structures with laminated facings", *Appl. Mech. Rev.* **50** (1997), 69–82.

[Anderson 2003] T. A. Anderson, "A 3-D elasticity solution for a sandwich composite with functionally graded core subjected to a transverse loading by a rigid sphere", *Compos. Struct.* **60**:3 (2003), 265–274.

[Apetre et al. 2002] N. A. Apetre, B. V. Sankar, and S. Venkataraman, "Indentation of a sandwich beam with functionally graded core", in *Proceedings of the 43rd AIAA/ASME/ASCE/AHS/ASC Structures, Structural Dynamics and Materials Conference* (Denver, CO, 2002), AIAA, Reston, VA, 22–25 April 2002. AIAA-2002-1683.

[Apetre et al. 2006] N. A. Apetre, B. V. Sankar, and D. R. Ambur, "Low-velocity impact response of sandwich beams with functionally graded core", *Int. J. Solids Struct.* **43**:9 (2006), 2479–2496.

[Carrera and Ciuffreda 2005] E. Carrera and A. Ciuffreda, "Bending of composites and sandwich plates subjected to localized lateral loadings: A comparison of various theories", *Compos. Struct.* **68**:2 (2005), 185–202.

[Corbett and Reid 1993] G. G. Corbett and S. R. Reid, "Local loading of simply-supported steel-grout sandwich plates", *Int. J. Impact Eng.* **13**:3 (1993), 443–461.

[Das et al. 2006] M. Das, A. Barut, E. Madenci, and D. R. Ambur, "A triangular plate element for thermo-elastic analysis of sandwich panels with a functionally graded core", *Int. J. Numer. Methods Eng.* **68**:9 (2006), 940–966.

[Frostig and Baruch 1996] Y. Frostig and M. Baruch, "Localized load effects in high-order bending of sandwich panels with flexible core", *J. Eng. Mech.* (*ASCE*) **122**:11 (1996), 1069–1076.

[Hohe and Librescu 2004] J. Hohe and L. Librescu, "Advances in the structural modeling of elastic sandwich panels", *Mech. Adv. Mater. Struct.* **11**:4–5 (2004), 395–424.

[Ichikawa 2001] K. Ichikawa (editor), *Functionally graded materials in the 21st century: A workshop on trends and forecasts* (Tsukuba, 2000), Kluwer, Dordrecht, 2001.

[Kirugulige et al. 2005] M. S. Kirugulige, R. Kitey, and H. V. Tippur, "Dynamic fracture behavior of model sandwich structures with functionally graded core: A feasibility study", *Compos. Sci. Technol.* **65**:7–8 (2005), 1052–1068.

[Koissin et al. 2004] V. Koissin, V. Skvortsov, S. Krahmalev, and A. Shilpsha, "The elastic response of sandwich structures to local loading", *Compos. Struct.* **63**:3–4 (2004), 375–385.

[Liew et al. 2004] K. M. Liew, J. Yang, and S. Kitipornchai, "Thermal post-buckling of laminated plates comprising functionally graded materials with temperature-dependent properties", *J. Appl. Mech.* (*ASME*) **71**:6 (2004), 839–850.

[Pollien et al. 2005] A. Pollien, Y. Conde, L. Pambaguian, and A. Mortensen, "Graded open cell aluminum foam core sandwich beams", *Mater. Sci. Eng. A* **404**:1–2 (2005), 9–18.

[Polyakov 2001] V. Polyakov, "Local effects at bending of nonsymmetric sandwich of composite and soft filler", *Compos. Struct.* **54**:2–3 (2001), 325–330.

[Reddy 1997] J. N. Reddy, *Mechanics of laminated composite plates: Theory and analysis*, CRC Press, Boca Raton, FL, 1997.

[Reddy 2000] J. N. Reddy, "Analysis of functionally graded plates", *Int. J. Numer. Methods Eng.* **47**:1–3 (2000), 663–684.

[Selvadurai 1979] A. P. S. Selvadurai, *Elastic analysis of soil-foundation interaction*, Developments in Geotechnical Engineering **17**, Elsevier, Amsterdam, 1979.

[da Silva and Santos 1998] L. A. P. S. da Silva and J. M. C. Santos, "Localised formulations for thick 'sandwich' laminated and composite structures", *Comput. Mech.* **22**:3 (1998), 211–224.

[Thomsen 1993] O. T. Thomsen, "Analysis of local bending effects in sandwich plates with orthotropic face layers subjected to localised loads", *Compos. Struct.* **25**:1–4 (1993), 511–520.

[Thomsen 1995] O. T. Thomsen, "Theoretical and experimental investigation of local bending effects in sandwich plates", *Compos. Struct.* **30**:1 (1995), 85–101.

[Türk and Fatt 1999] M. H. Türk and M. S. H. Fatt, "Localized damage response of composite sandwich plates", *Compos. B Eng.* **30**:2 (1999), 157–165.

[Venkataraman and Sankar 2003] S. Venkataraman and B. V. Sankar, "Elasticity solution for stresses in a sandwich beam with functionally graded core", *AIAA J.* **41**:12 (2003), 2501–2505.

[Venkataraman et al. 2004] S. Venkataraman, R. T. Haftka, B. V. Sankar, H. Zhu, and M. L. Blosser, "Optimal functionally graded metallic foam thermal insulation", *AIAA J.* **42**:11 (2004), 2355–2363.

[Weissman-Berman et al. 1996] D. Weissman-Berman, S. Lahiri, and R. Marrey, "Flexural response of sandwich plates with core as elastic foundation", *Trans. Soc. Naval Arch. Marine Eng.* **104** (1996), 491–518.

[Yang and Shen 2003a] J. Yang and H. S. Shen, "Non-linear analysis of functionally graded plates under transverse and in-plane loads", *Int. J. Non-Linear Mech.* **38**:4 (2003), 467–482.

[Yang and Shen 2003b] J. Yang and H. S. Shen, "Nonlinear bending analysis of shear deformable functionally graded plates subjected to thermo-mechanical loads and under various boundary conditions", *Compos. B Eng.* **34**:2 (2003), 103–115.

[Yang et al. 2001] J. Yang, H. S. Shen, and L. Zhang, "Nonlinear local response of foam-filled sandwich plates with laminated faces under combined transverse and in-plane loads", *Compos. Struct.* **52**:2 (2001), 137–148.

[Zhu and Sankar 2007] H. Zhu and B. V. Sankar, "Analysis of sandwich TPS panel with functionally graded foam core by Galerkin method", *Compos. Struct.* **77**:3 (2007), 280–287.

JIE YANG: j.yang@rmit.edu.au
School of Aerospace, Mechanical and Manufacturing Engineering, RMIT University, PO Box 71, Bundoora, VIC 3083, Australia

SRITAWAT KITIPORNCHAI: bcskit@cityu.edu.hk
Department of Building and Construction, City University of Hong Kong, Tat Chee Avenue, Kowloon, Hong Kong

KIM MEOW LIEW: kmliew@cityu.edu.hk
Department of Building and Construction, City University of Hong Kong, Tat Chee Avenue, Kowloon, Hong Kong